Progress In Electromagnetics Research Letters, Vol. 104, 95–103, 2022

Low Sidelobe and Tilted Beam Microstrip Antenna for Circularly-Polarized SAR Onboard UAV

Yohandri[1, *], Asrizal[1], Asif Awaludin[2], and Josaphat T. Sri Sumantyo[3]

Abstract—This work is purposed to provide microstrip antennas for a CP-SAR system with low sidelobe, tilted beam, and circular polarization. This antenna is configured for the L-band (1.27 GHz) mounting on an Unmanned Aerial Vehicle (UAV). The proposed microstrip antenna consists of three-square radiating elements, due to the ease in fabrication. Meanwhile, the proximity structure has been adopted in the feeding network. The tilted beam was obtained by arranging the different phases for each element. On the other hand, a low sidelobe was achieved by managing the power distribution of each patch using the Chebyshev polynomial. The proposed antenna was precisely printed and examined in an anechoic chamber to verify the characteristics of the antenna such as polarization, sidelobe level, and beam direction. Based on the measurement results, the proposed antenna has a tilted beam and a low side lobe that meets the specifications of the CP-SAR system.

1. INTRODUCTION

Synthetic-Aperture Radar (SAR) is one of the powerful technologies that can be used in wide range of fields [1, 2]. Various researches are continually underway to improve SAR capabilities in both hardware [3] and data processing technology [4]. The latest technology in SAR is Circularly Polarized SAR (CP-SAR) [5]. This technology allows the transmission and reception of electromagnetic waves in circular polarization. Due to its characteristics, the SAR with circular polarization has been extensively studied. In addition, circular polarization is an advantageous way of transmitting electromagnetic waves due to the ability to minimize propagation errors [6] and cross-polarization [7, 8]. The CP-SAR has detailed information compared to linear polarization (LP-SAR) such as tilting angle, ellipticity, and axial ratio [3]. This parameter reveals more detailed information the CP-SAR sensor acquires. In addition, circular polarization is not affected by the rotational effect of Faraday, as electromagnetic waves propagate in the ionosphere [9]. On the basis of its advantages, the Josaphat Microwave and Remote Sensing Laboratory (JMRSL) is developing a CP-SAR system for UAVs. The CP-SAR system is targeted for a variety of purposes, such as disaster monitoring, land cover, forest, and fire mapping. A photograph of our UAV for CP-SAR is shown in Figure 1.

A number of circular polarization antennas have been developed [10, 11]. However, the developed antenna did not comply with the CP-SAR specifications for UAV such as low sidelobe and tilted beam. In our previous work, a circularly polarized microstrip antenna for UAV has been developed [12, 13]. Mostly, the developed antenna generates radiation perpendicular to the theta plane. The antenna is therefore mounted on the side body of the UAV to meet the side-looking radar requirement. As a result, a load balancer is required on the other side of UAV as shown in Figure 2(a). The aircraft was made

Received 28 March 2022, Accepted 17 May 2022, Scheduled 31 May 2022

* Corresponding author: Yohandri (yohandri@fmipa.unp.ac.id).

[1] Physics Department, Faculty of Mathematics and Natural Science, Universitas Negeri Padang, Jl. Prof. Hamka, Padang, Sumatera Barat 25131, Indonesia. [2] Center for Atmospheric Science and Technology, National Institute of Aeronautics and Space, Jl. dr. Djundjunan 133, Bandung 40173, Indonesia. [3] Josaphat Microwave Remote Sensing Laboratory, Center for Environmental Remote Sensing, Chiba University, 1-33 Yayoi-cho, Inage-ku, Chiba 263-8522, Japan.

Figure 1. Photograph of our UAV for CP-SAR having total length 4.75 m, wingspan 6 m, and maximum payload 25 kg.

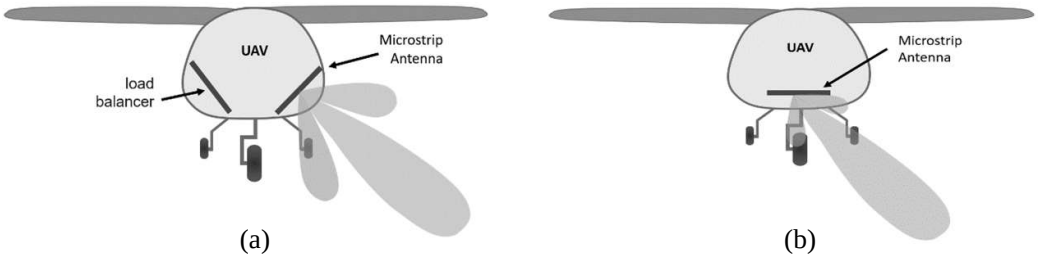

Figure 2. Illustration of installation of microstrip antenna, (a) previous antenna on the side of UAV with load balancer and (b) low sidelobe and tilted beam antenna on the bottom of UAV and no-load balancer required.

heavier by a load balancer which occupies the space inside the UAV. Consequently, heavier UAV needs a more powerful engine and fewer sensors that the UAV can carry. Moreover, the sidelobe level of the antenna was less satisfactory for the CP-SAR system [14]. In that case, high sidelobe produces errors when a backscattering signal is collected.

To overcome this problem, the antenna has to be installed at the bottom of the UAV while keeping radiation sideways and low sidelobe as illustrated in Figure 2(b). The circular polarization antenna was constructed using a three simple square microstrip antenna with corner truncated since it is easy to fabricate. Meanwhile, the proximity feed method is used to power the antenna. The proximity feed has an advantage as it can increase the antenna bandwidth [15]. The power distribution of each patch is regulated using the Chebyshev polynomial to achieve a low sidelobe antenna. On the other hand, the tilted beam was formulated using the principle of phased array [16].

The purpose of this work is to realize an array of microstrip antenna for UAV, which has a circular polarization, low sidelobe, and tilted beam. This proposed antenna will be installed on the bottom of the UAV. The antenna analysis and design will be presented in Section 2. Moreover, method and antenna performance are discussed in Sections 3 and 4, respectively.

2. DESIGN OF PROPOSED ANTENNA

A CP-SAR system has several devices, one of which is antenna. Antennas are important components which act as transmitters and receivers in the CP-SAR system. Table 1 displays the main parameters of antenna for CP-SAR installed aboard UAV.

The antenna was designed for uniform space ($d = \lambda_0/2$) at the level of sidelobe of 20 dB. The Array Factor (AF) can be formulated as [17] for array antenna with three patches ($P = 3$, $M = 1$).

$$AF(u) = a_1 + a_2 \cos 2u \tag{1}$$

Table 1. The main parameters of antenna for CP-SAR installed aboard UAV.

Parameters	Specification
Working Frequency (GHz)	1.27 (L-Band)
Axial ratio (dB)	≤ 3
Elevation beam width	3.57°–31.02°
Polarization (Tx/Rx)	RHCP or LHCP
Sidelobe level	> 15 dB

where $u = 2\pi(d/\lambda)\cos\theta$, and u can be simplified for uniform spaces ($d = \lambda/2$) as $u = \pi\cos\theta$. The excitation coefficient (a_1 and a_2) can be achieved by applying the polynomial of Chebyshev, and AF is defined as.

$$AF(u) = 0.5 + 0.61\cos 2u \tag{2}$$

Furthermore, the equation of the array factor was applied to calculate the power of each antenna patch. The power distribution of each patch was managed over the feed network. Figure 3 depicts the power comparison on each patch normalized to the center of the element.

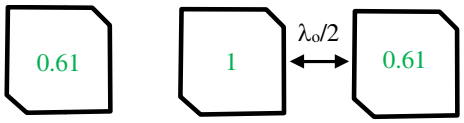

Figure 3. Illustration of power comparison for each patch of the antenna.

On the pattern of radiation, the main beam was tilted to 12 degrees to comply the CP-SAR specification. There are various methods which can be adopted for tilted beam [18, 19]. The simple method used in this proposed antenna was phase shifting. Phase sifting was done in the feeding network by controlling the additional feed line length (ΔL).

The proposed antenna geometry consists of the elements of the radiator and feed networks. The three square microstrip antenna patches with corner truncated were implemented in this design. In addition, a proximity feed method was implemented in the feed network. Figure 4 displays the power divider (T-junction) for the distribution of the power on each element of the radiator.

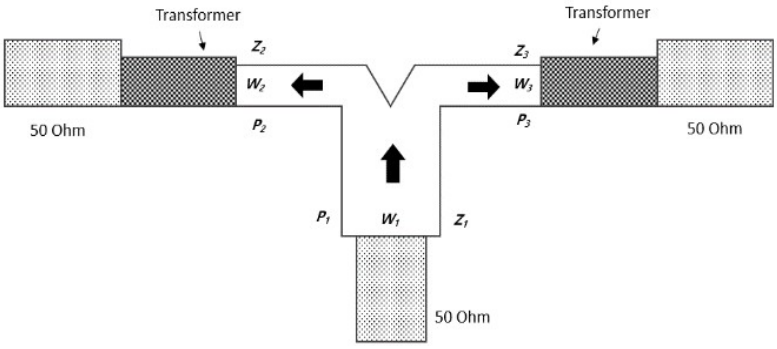

Figure 4. Power divider (T-Junction) with impedance matching (transformer).

Figure 4 depicts the division of input power into two outputs. The input power P_1 is sent to the junction through a microstrip line with an impedance Z_1 and width W_1. In addition, the power P_1 was split into two parts, namely P_2 and P_3. The width and impedance of P_2 and P_3 are W_2, Z_2, and W_3, Z_3, respectively.

The feed network in the proposed antenna was designed to be based on the distribution of power. Two T-junction (A and B) power dividers were used to distribute the power as shown in Figure 5. The power division ratio for the A and B junctions is shown in Table 2.

Table 2. The ratio of the power dividing for A and B junction.

Junction	P_2	P_3	Ratio (P_3/P_2)
A	1.61	0.61	0.38
B	0.61	1	0.61

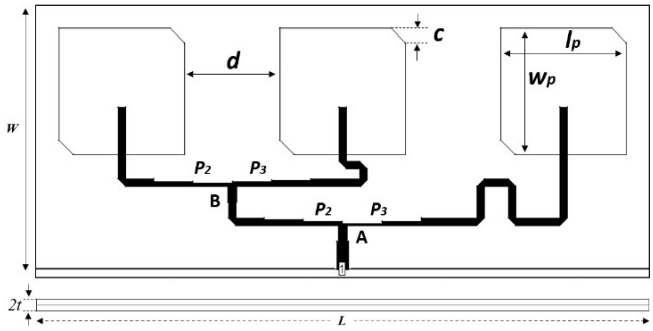

Figure 5. The geometry design of the low sidelobe and tilted beam microstrip array antenna consists of three elements and proximity feeding network.

3. METHOD

Simulation is done over 2 layers of geometry design as shown in Figure 5. In the design of the low sidelobe and the tilted beam antenna, a finite ground plane model using the MoM was used. The optimum designs are then precisely manufactured to ensure that the characteristics of the manufactured antenna comply with the simulated model. A Nippon Pillar (NPC-H220A) substrate with a thickness of 1.6 mm was selected to print the antenna. This substrate has a tangent loss of 0.0005 and a dielectric constant of 2.17. In this design, the antenna was printed using two layers of substrate. Three radiators were printed on the upper layer of the substrate and the proximity feed network on the lower layer.

The printed antenna was then investigated to determine its characteristics. The Vector Network Analyzer (Agilent, E5062A) was operated to measure the coefficient of reflection and the voltage constant wave ratio (VSWR). Meanwhile, radiation patterns and axial ratio were characterized in an anechoic chamber (Figure 6) having dimensions of $4 \times 8.5 \times 2.4\,\mathrm{m}^3$.

Standard references consisting of a dipole antenna and a conical log spiral (RHCP and LHCP) were used for characterization. The Antenna Under Test (AUT) was placed on a rotary table. The turntable can precisely adjust the rotation of the antenna to determine the pattern of radiation. Moreover, the speed and direction of the rotary table were adjusted using a controller from outside the chamber. The frequency, power, and angle of radiation can be adjusted on a computer.

4. RESULTS AND DISCUSSION

The proposed antenna was printed on two layers. The top layer is three square radiators, and the bottom layer is a feeder. The two layers of the antenna are assembled and pressed using plastic bolts. Figure 7 shows a photograph of the low sidelobe and tilted beam microstrip antenna. The array antenna was printed on the basis of optimum simulation parameters. Table 3 shows a list of the best parameters

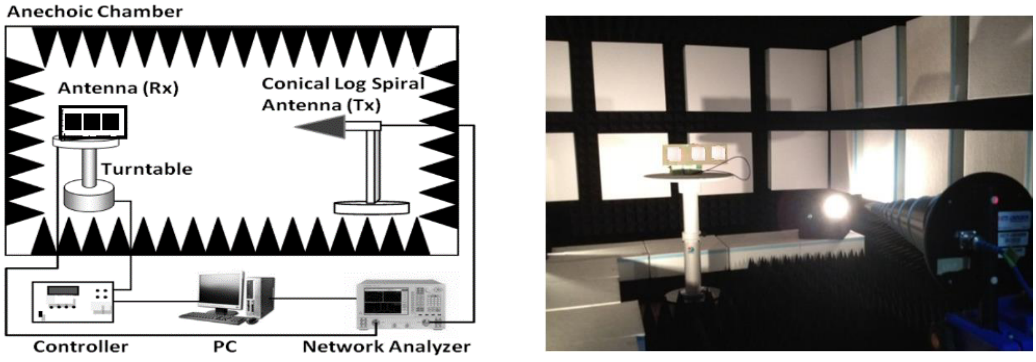

Figure 6. The antenna under test, (a) measurement system Schematic, (b) photograph.

Figure 7. Printed antenna on two layers of Nippon Pillar (NPC-H220A).

Table 3. Geometry parameters (mm) of low sidelobe and tilted beam microstrip array antenna.

Parameters	Size (mm)
L	379.47
W	185.07
t	1.600
$w_p,\ l_p$	79.20
d	53.97
c	9.120

of the antenna and the size (mm). In addition, the measured characteristics of the antenna were plotted along with the simulation data.

The properties of the antenna, such as the coefficient of reflection (S_{11}), VSWR, axial ratio (AR), and the pattern of radiation, are shown in Figures 8–12. The simulation and measurement coefficients of reflection (S_{11}) are shown in Figure 8. The minimum coefficients of reflection for measured and simulated results are -15.6 dB and -26.74 dB, respectively. In addition, the simulated and measured bandwidths at -10 dB are 4.8% and 5.6% with respect to the 1.27 GHz frequency center.

In general, the simulated and measured coefficients of reflection are in good agreement. The working frequency is, however, shifted slightly to a higher frequency. The slight shift in frequency is likely because the printed patches are slightly smaller than the simulation size. In principle, the smaller the patch antenna size is, the higher the working frequency is [20]. Moreover, the measured antenna bandwidth is slightly wider (0.8%) than the simulation results. The wider width of the measuring bandwidth is

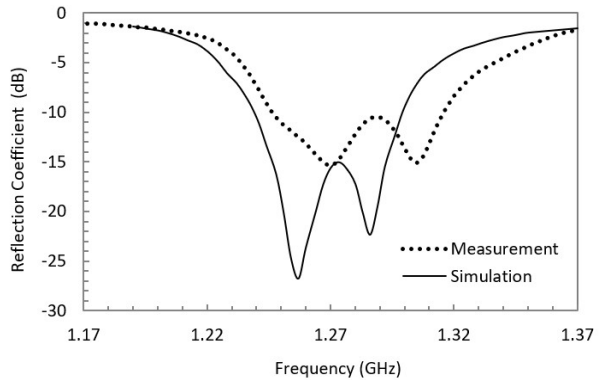

Figure 8. The relationship between simulation and measurement coefficient of reflection and frequency.

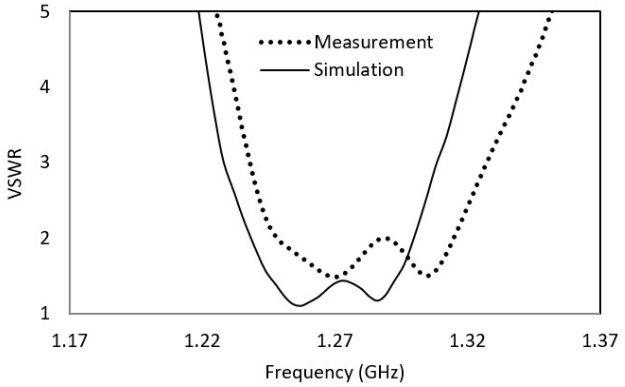

Figure 9. Simulation and measurement VSWR of the antenna.

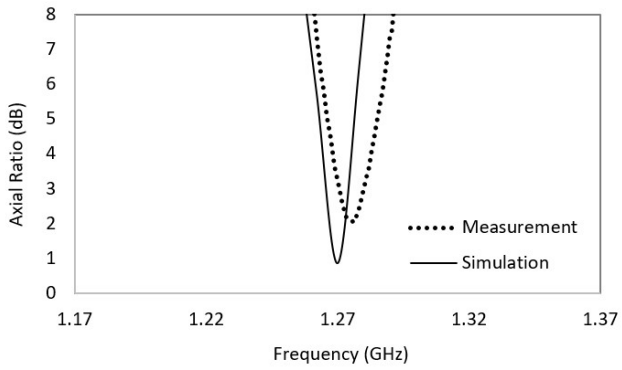

Figure 10. Simulation and measurement result of the axial ratio (AR).

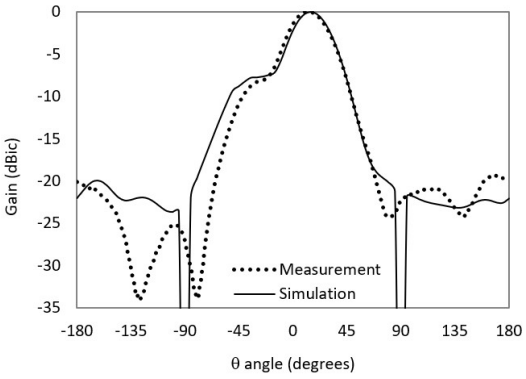

Figure 11. Simulation and measurement of normalized radiation pattern of the proposed antenna at frequency 1.27 GHz.

suspected due to the presence of an air gap between the substrate layers [21].

Figure 9 shows the effect of the frequency on the simulation and measurement of VSWR. Apparently, the simulation and measurement results are in good agreement. The measured and simulated impedance bandwidths (VSWRs) are 5.31% and 4.80%, respectively. The measured VSWR at the working frequency (1.27 GHz) is 1.48, and the simulated VSWR is 1.40. In short, the simulation and measurement results show high compatibility and a high matching between the feeding network and antenna [22].

The polarization characteristics of the antenna are determined by axial ratio (AR). The antenna must have a maximum axial ratio of 3 dB for circular polarization [23]. Figure 10 shows the relationship between the axial ratio of the proposed antenna and the frequency. The bandwidth of measured axial ratio (3-dB) is 9.75 MHz (0.76%). Meanwhile, the axial ratio bandwidth in the simulation is 13.6 MHz (1.07%) with a lower axial ratio of 0.85 dB at a frequency of 1.27 GHz. The operating frequency of the measurement shifts slightly to higher frequencies. This is due to slight imperfections in the fabrication process that make the printed antenna smaller than the simulation size [20]. Subsequently, measured axial ratio looks higher than the simulation. This result is caused by the smaller corner-truncation at the printed square patch than the simulation configuration [24].

The level of the sidelobe antenna can be shown in the normalized patterns of radiation as seen in Figure 11. The radiation pattern is plotted as a function of the theta on the theta plane. On the measured radiation pattern, the sidelobe appears on $\theta = -98^\circ$ and $\theta = +118^\circ$ with peaks of -25.13 dB and -21.07 dB, respectively. Meanwhile, the simulated radiation pattern shows the sidelobe

at $\theta = -120°$ and $\theta = +165°$ with peaks of -22.11 dB and -22.35 dB, respectively.

Generally, the simulation and measurement results of the radiation pattern are in good agreement. A slight difference in the pattern of radiation can be attributed to imperfections in the characterization process, such as a small shift when the antenna is rotated on the turntable. Nevertheless, the difference between the main lobe and sidelobe of the fabricated antenna is 25.13 dB and 21.07 dB for $\theta = -98°$ and $\theta = +118°$, respectively. Based on this sidelobe level it can be concluded that the developed antennas can be used and meet the antenna requirements for CP-SAR onboard UAV [25].

The printed antenna, on the other hand, has the tilted main beam as shown in Figure 12. In this graph, the main beam antenna is tilted at $\theta = +12°$. This angle complies with the required CP-SAR antenna specifications, which are between 3.57° and 31.02° [25]. Moreover, the beamwidth of the antenna is bit wide due to the limited number of patches [26].

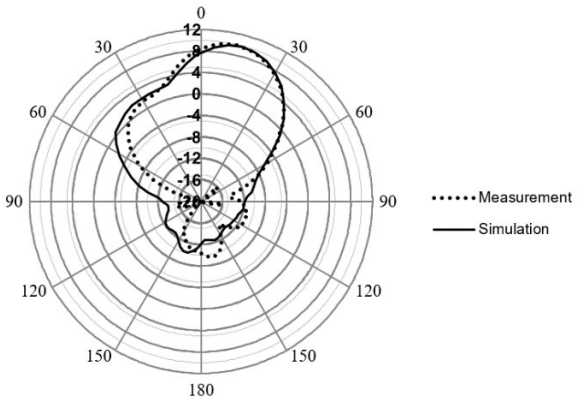

Figure 12. Antenna polarization at frequency 1.27 GHz.

Based on the antenna's characteristics in terms of reflection coefficient, axial ratio, low sidelobe, and tilted beam, the developed antenna meets the CP-SAR required specification. Table 4 presents the comparison of some of the previous antennas and the proposed antenna.

Table 4 shows the performance of other work (CP antenna for satellite and Ultra-lightweight antenna) as compared to the proposed array antenna. The CP antenna for satellite has a sidelobe level varied from 16.6 to 20 dB with 0° beam direction. On the other hand, the ultra-light weight antenna has a sidelobe of 20 dB and 0° beam direction. The proposed antenna has a sidelobe of 21.07 dB and a tilted beam of 12°.

Table 4. Comparison of several previous antennas with proposed antenna.

Antenna	Beam Direction	Sidelobe (dB)
CP antenna for satellite [27]	0°	16.6–20
Ultra-lightweight antenna [28]	0°	20
Proposed Array antenna	12°	21.07

5. CONCLUSION

The development of a low sidelobe and tilted beam microstrip array antenna has been presented in this paper. The simulation and measurement results show a good agreement. In general, the performances of the proposed antenna in terms of coefficient of reflection, and axial, sidelobe level, and tilted beam satisfy the requirements of CP-SAR system. The proposed antenna has a low sidelobe level of 20 dB. Moreover, the main radiation beam antenna can be tilted to 12°. With its good performance, this circularly polarized antenna can be installed beneath a UAV for a variety of CP-SAR missions.

ACKNOWLEDGMENT

The authors would like to thank Directorate General of Higher Education (DIKTI), Ministry of Research, Technology and Higher Education, Indonesia, for the Research Grant.

REFERENCES

1. Owusu Twumasi, J., P. DeStefano, and J. T. Christian, "The application of synthetic aperture radar imaging technique to measure moisture content of concrete structures," *Meas. J. Int. Meas. Confed.*, Vol. 152, 107335, 2020.
2. Tanase, M. A., et al., "Synthetic aperture radar sensitivity to forest changes: A simulations-based study for the Romanian forests," *Sci. Total Environ.*, Vol. 689, 1104–1114, 2019.
3. Tetuko, J., et al., "Development of circularly polarized synthetic aperture radar on-board UAV JX-1," *Int. J. Remote Sens.*, 4762–4765, 2017.
4. Schwegmann, C. P., W. Kleynhans, B. P. Salmon, L. W. Mdakane, and R. G. V. Meyer, "Very deep learning for ship discrimination in Synthetic Aperture Radar imagery," *International Geoscience and Remote Sensing Symposium (IGARSS)*, 104–107, 2016.
5. Sumantyo, J. T. S. and K. V. Chet, "Development of circularly polarized synthetic aperture radar onboard UAV for earth diagnosis," *Proceedings of the European Conference on Synthetic Aperture Radar, EUSAR*, 2012.
6. Brookner, E., W. M. Hall, and R. H. Westlake, "Faraday loss for L-band radar and communications systems," *IEEE Trans. Aerosp. Electron. Syst.*, Vol. 21, No. 4, 459–469, 1985.
7. Yahya, M. and Z. Awang, "Cross polarization ratio analysis of circular polarized patch antenna," *Proc. — 2010 12th Int. Conf. Electromagn. Adv. Appl. ICEAA'10*, 442–445, 2010.
8. Fukusako, T., "Broadband characterization of circularly polarized waveguide antennas using L-shaped probe," *J. Electromagn. Eng. Sci.*, Vol. 17, No. 1, 1–8, 2017.
9. Rignot, E. J. M., "Effect of Faraday rotation on L-band interferometric and polarimetric synthetic-aperture radar data," *IEEE Trans. Geosci. Remote Sens.*, 383–390, 2000.
10. Baharuddin, M., V. Wissan, J. Tetuko Sri Sumantyo, and H. Kuze, "Elliptical microstrip antenna for circularly polarized synthetic aperture radar," *AEU — Int. J. Electron. Commun.*, Vol. 65, No. 1, 62–67, 2011.
11. Shookooh, B. R., A. Monajati, and H. Khodabakhshi, "Theory, design, and implementation of a new family of ultra-wideband metamaterial microstrip array antennas based on fractal and fibonacci geometric patterns," *J. Electromagn. Eng. Sci.*, Vol. 20, No. 1, 53–63, 2020.
12. Yohandri, V. Wissan, I. Firmansyah, P. Rizki Akbar, J. T. Sri Sumantyo, and H. Kuze, "Development of circularly polarized array antenna for synthetic aperture radar sensor installed on UAV," *Progress In Electromagnetics Research C*, Vol. 19, 119–133, 2011.
13. Hussein, M., Yohandri, J. T. S. Sumantyo, and A. Yahia, "A low sidelobe level of circularly polarized microstrip array antenna for CP-SAR sensor," *Journal of Electromagnetic Waves and Applications*, Vol. 27, No. 15, 1931–1941, Oct. 2013.
14. Yohandri, J. T. Sri Sumantyo, and H. Kuze, "Circularly polarized array antennas for synthetic aperture radar," *PIERS Proceedings*, 1244–1247, Suzhou, China, Sep. 12–16, 2011.
15. Varshney, H. K. M. Kumar, A. K. Jaiswal, R. Saxena, and K. Jaiswal, "A survey on different feeding techniques of rectangular microstrip patch antenna," *Int. J. Curr. Eng. Technol.*, Vol. 4, No. 3, 1418–1423, 2014.
16. Clay, A. C., S. C. Wooh, L. Azar, and J. Y. Wang, "Experimental study of phased array beam steering characteristics," *J. Nondestruct. Eval.*, Vol. 18, 59–71, 1999.
17. Balanis, C. E., *Antenna Theory: Analysis and Design*, 3rd Edition, C. A. Balanis, 1136, 2005.
18. Kim, J. O., W. S. Yoon, and S. M. Han, "Frequency-selective beamforming array antenna systems with frequency-dependent phase shifters," *J. Electromagn. Eng. Sci.*, Vol. 19, No. 4, 259–265, 2019.

19. Lee, S. G. and J. H. Lee, "Calculating array patterns using an active element pattern method with ground edge effects," *J. Electromagn. Eng. Sci.*, Vol. 18, No. 3, 175–181, 2018.
20. Lee, K. F. and K. F. Tong, "Microstrip patch antennas," *Handbook of Antenna Technologies*, 2016.
21. Verma, R. K., N. K. Saxena, and P. K. S. Pourush, "Effect of air-gap technique in bandwidth of microstrip patch array antenna," *Int. J. Res. Publ. Eng. Technol. [IJRPET]*, Vol. 3, No. 6, 165–168, 2017.
22. Arora, A., A. Khemchandani, Y. Rawat, S. Singhai, and G. Chaitanya, "Comparative study of different feeding techniques for rectangular microstrip patch antenna," *Int. J. Innov. Res. Electr. Electron. Instrum. Control Eng.*, Vol. 3, No. 5, 2–35, 2015.
23. Garg, R., P. Bhartia, I. Bahl, and A. Ittipiboon, *Microstrip Antenna Design Handbook*, 2001.
24. Gautam, A. K., P. Benjwal, and B. K. Kanaujia, "A compact square microstrip antenna for circular polarization," *Microw. Opt. Technol. Lett.*, Vol. 54, No. 4, 897–900, 2012.
25. Rizki Akbar, P., J. T. S. Sumantyo, and H. Kuze, "CP-SAR UAV Development," *International Archives of the Photogrammetry, Remote Sensing and Spatial Information Science*, Vol. XXXVIII, Part 8, 203–208, 2010.
26. Bevelacqua, P. J. and C. Balanis, "Antenna arrays: Performance limits and geometry optimization," 158 pages, Arizona State Univ., 2008.
27. Alieldin, A., Y. Huang, M. Stanley, and S. Joseph, "A circularly polarized circular antenna array for satellite TV reception," *2018 15th Eur. Radar Conf. EuRAD 2018*, 505–508, 2018.
28. Huang, J., W. Lin, F. Qiu, C. Jiang, D. Lei, and Y. J. Guo, "A low profile, ultra-lightweight, high efficient circularly-polarized antenna array for Ku band satellite applications," *IEEE Access*, Vol. 5, 18356–18365, 2017.